UV Coronal Emission for Beginners v.1.1

S. Giordano

Rapporto nr.129   22/03/2010

UV Coronal Emission for Beginners v.1.1

Silvio Giordano – March 22, 2010 - `uv_emission_v1.1.tex`

Istituto Nazionale di Astrofisica (INAF), Osservatorio Astronomico di Torino

Contents

1. Abstract

This report presents a basic description of the physical mechanisms and relative formulas for the UV emission from solar corona. It is mainly focused on the H I Lyα 1216 and O VI 1032/1038 doublet spectral lines observed by UVCS aboard SOHO. Some elements for diagnostics of electron density and abundances are presented. On the basis of present formulation the expected He II 304 intensity is preliminarily computed.

2. Radiative component

The radiative component of an emission line in the solar corona is due to the resonant scattering of the disk radiation by coronal ions/atoms, the physical mechanism is represented in figure 1 (upper). The total intensity (*photons* cm^{-2} s^{-1} sr^{-1}) by following Noci, Kohl and Withbroe (1987); Noci et al. (1993), can be written as

$$I_r = \frac{b \, B_{12} \, h \, \lambda_0}{4\pi} \int_{l.o.s} n_i \, dl \int_\Omega p(\phi) \, d\omega \int_0^{+\infty} I_{ex}(\lambda - \delta\lambda) \, \Phi(\lambda, \mathbf{n}') \, d\lambda \ , \tag{1}$$

where: b is the branching ratio of considered transition (*adimensional*), h is the Planck constant (*erg s*), λ_0 is the reference wavelength of the transition (*cm*), n_i is the numerical ion/atom density (cm^{-3}), $p(\phi)$ takes into account the geometry of the scattering process, ϕ is the angle between the direction of the incident radiation $\mathbf{n}'$ and the line–of–sight (l.o.s.). $I_{ex}(\lambda - \delta\lambda)$ is the intensity spectrum (*photons* cm^{-2} s^{-1} sr^{-1} cm^{-1}) of incident radiation from lower atmosphere, $\delta\lambda$ is the shift of this profile with respect to the reference profile due to the outflow velocity, $\mathbf{w}$, of coronal absorbing ions/atoms in the direction $\mathbf{n}'$:

$$\delta\lambda = \frac{\lambda_0}{c} \, \mathbf{w} \, \cdot \, \mathbf{n}' \ . \tag{2}$$

$\Phi(\lambda, \mathbf{n}')$ is the normalized coronal absorption profile along the direction of the incident radiation, which can be assumed to be gaussian in the assumption of a maxwellian velocity distribution of the absorbing particles

$$\Phi(\lambda, \mathbf{n}') = \frac{1}{\sigma_\lambda(\mathbf{n}') \, \sqrt{2\pi}} \, \exp \left[-\frac{1}{2} \left(\frac{\lambda - \lambda_0}{\sigma_\lambda(\mathbf{n}')} \right)^2 \right] \quad (cm^{-1}), \tag{3}$$

where $\sigma_\lambda(\mathbf{n}')$ is the standard deviation of the absorption profile related to the kinetic temperature $T_{\mathbf{n}'}$ along the direction of the incident radiation

$$\sigma_\lambda(\mathbf{n}') = \frac{\lambda_0}{c} \, \sqrt{\frac{k_B \, T_{\mathbf{n}'}}{m_p \, A}} \quad (cm), \tag{4}$$

where: c is the light speed (cm s^{-1}), k_B is the Boltzmann constant (erg K^{-1}), m_p is the proton mass (g), A is the ion mass number (*adimensional*),

In order to obtain the total radiation emitted by resonant scattering we integrate along the l.o.s, dl, over the solid angle subtended by the source of exciting radiation, $d\omega$, and the product between the incident and absorption profile is integrated over the wavelength, $d\lambda$.

B_{12} is the Einstein coefficient for stimulated emission, the values of this coefficient are computed for considered transitions following Rybicki and Lightman (1979); Foukal (1990):

$$B_{12} \;=\; \frac{4\pi^2 e^2}{h\nu_0 m_e c} \, f_{12} \;=\; \frac{4\pi^2 e^2 \lambda_0}{h m_e c^2} \, f_{12} \quad (cm^2 \ erg^{-1} \ s^{-1}), \tag{5}$$

where: f_{12} is the atomic oscillator strength (*adimensional*), e is the electron charge (*Stat-Coulomb*), m_e is the electron mass (g), ν_0 is the reference frequency of the transition $\nu_0 = c/\lambda_0$ (s^{-1}).

Note: Lang (1978) defines the Einstein coefficient as

$$B_{12,Lang} \; = \; \frac{\pi e^2}{m_e E_{12}} \, f_{12} \; ,$$

where $E_{12} = h\nu_0$, therefore the relation between this definition and equation 5 is

$$B_{12} \; = \; \frac{4\pi}{c} \, B_{12,Lang} \; .$$

The physical constants are reported in Table 1 and the atomic parameters in Table 2.
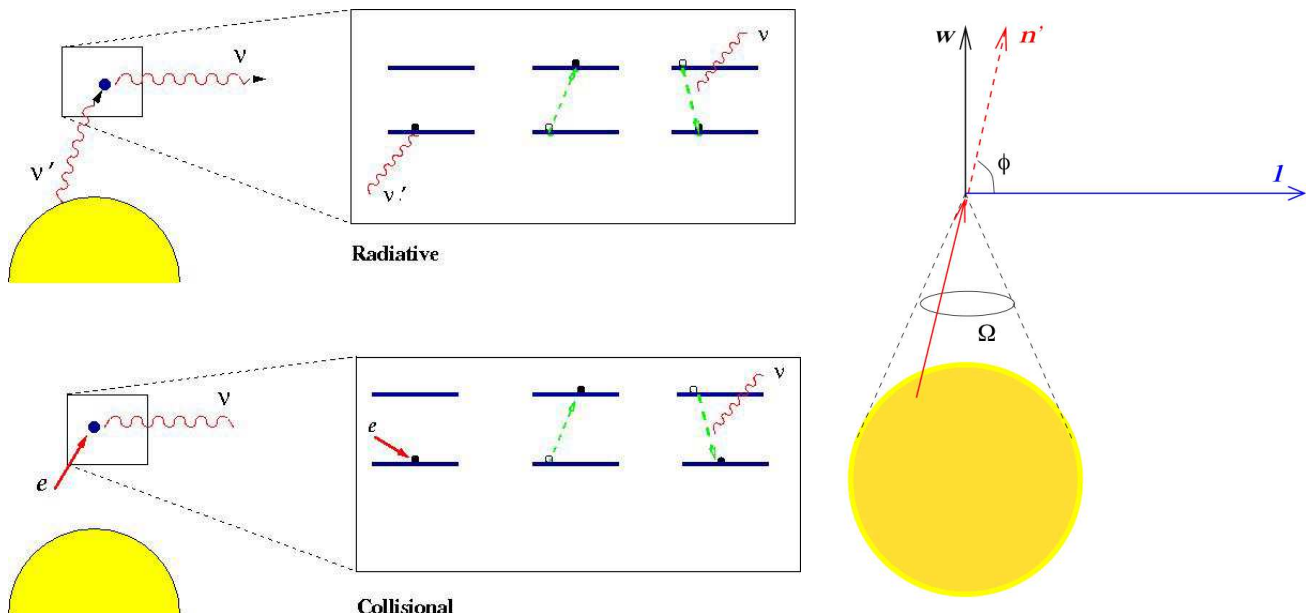

Fig. 1.— Left: Resonant (upper) and Collisional (lower) Scattering processes. Right: Geometry of the resonant scattering process.

Table 1: Physical Constants

Constant	Symbol	Value	
Speed of Light	c	2.9979×10^{10}	$cm \; s^{-1}$
Planck constant	h	6.6261×10^{-27}	$erg \; s$
Boltzmann constant	k_B	1.3807×10^{-16}	$erg \; K^{-1}$
Proton mass	m_p	1.6725×10^{-24}	g
Electron mass	m_e	9.1091×10^{-28}	g
Electron charge	e	4.8000×10^{-10}	$StatCoulomb$

3. Collisional component

The physical mechanism producing the collisional component of an emission line in the solar corona is the excitation of a coronal ion/atom by collision with a free electron. This process

Table 2: Atomic Parameters of Considered Transitions

Spectral Line	λ_0 (Å) (*)	ν_0 10^{15} (s^{-1})	f_{12}	B_{12} 10^9 (**)	b	A
H I Lyα	1215.67	2.46605	0.4162	8.4838	1	1
H I Lyβ	1025.72	2.92273	0.0791	1.3604	0.88	1
H I Lyγ	972.50	3.08267	0.0290	0.4729	1 ?	1
O VI 1032	1031.91	2.90519	0.1310	2.2667	1	16
O VI 1037	1037.61	2.88924	0.0648	1.1274	1	16
S XII 499	499.37	6.00336	0.0730	0.6112	1 ?	28
S XII 521	520.66	5.75788	0.0350	0.3056	1 ?	28
He II 304	304.78	9.83627	0.4162	2.1021	1	4

* 1Å$=10^{-8}$cm

** cm^{2}erg^{-1}s^{-1}

is represented in figure 1 (lower). Following Noci, Kohl and Withbroe (1987), the total intensity ($photons\ cm^{-2}\ s^{-1}\ sr^{-1}$) of the collisional component of a coronal line can be written as

$$I_c = \frac{b}{4\pi} \int_{l.o.s} n_e\ n_i\ q_{coll}\ dl \ , \tag{6}$$

where: n_e is the electron density (cm^{-3}), q_{coll} is the collisional coefficient (Noci, Kohl and Withbroe 1987) (or Seaton 64 ?),

$$q_{coll} = 2.73\ \times\ 10^{-15}\ T_e^{-\frac{1}{2}}\ (E_{12})^{-1}\ f_{12}\ \bar{g}\ \exp^{-\frac{E_{12}}{k_B T_e}}\quad (cm^3\ s^{-1}), \tag{7}$$

where: T_e is the electron temperature (K), E_{12} is the transition energy $E_{12} = h\nu_0 = hc/\lambda_0$ (erg), $\bar{g}$ is Gaunt factor computed by using Mewe (1972) approximation. The code used to compute the collisional coefficient is *qcoll.pro* in the directory $HOME/PRO/UV_CODE/PRO_DEV.

4. Radiative component approximations

The functions $p(\phi)$, which take into account the geometry of the resonant scattering, for the spectral lines of interest have been calculated by Beckers and Chipman (1974): for HI Lyα line: $p(\phi) = (1/4\pi)\ (11 + 3\cos^2\phi)/12$, for O VI 1032 line: $p(\phi) = (1/4\pi)\ (7 + 3\cos^2\phi)/8$, for O VI 1037 line: $p(\phi) = 1/4\pi$.

Because of the scattering angle, ϕ, is close to 90°, the value of $p(\phi)$ can be approximated to $1/4\pi$ with an uncertainty no more than 7% for HI Lyα and no more than 10% for O VI 1032 (Figure 3). Therefore we use the following approximation

$$\int_\Omega p(\phi)\,d\omega\ \sim\ \frac{1}{4\pi}\ \Omega \ , \tag{8}$$

The solid angle subtended by the source of resonant radiation at distance r from Sun center is computed (Noci, Kohl and Withbroe 1987) as

$$\Omega\ =\ 2\pi\ \left(1 - \sqrt{1 - \frac{1}{x^2}}\right) , \tag{9}$$

where $x = r/R_\odot$ is the heliocentric distance in solar radii units (*adimensional*).
Note: At large heliocentric distances, $r \gg R_\odot$, the solid angle can be approximated by $\Omega \sim \pi/x^2$, see also Table 3.

Table 3: Solid Angle Approximations

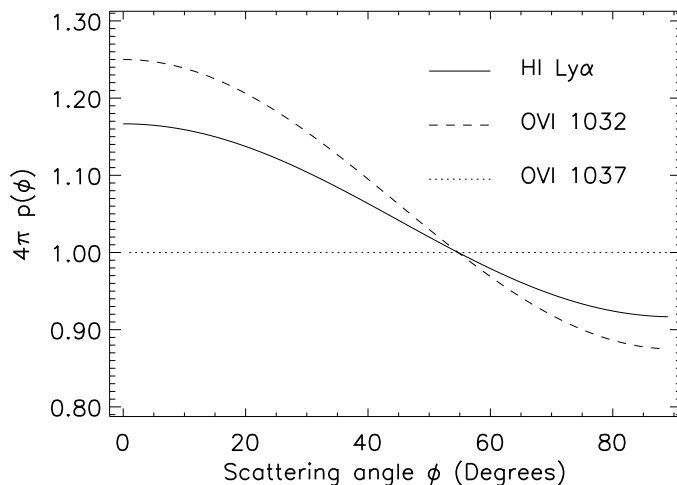| x	Ω	$\Omega \sim \pi/x^2$	Ratio
1.50	1.60	1.40	1.14
1.75	1.13	1.03	1.10
2.00	0.84	0.78	1.08
3.00	0.36	0.35	1.03

Fig. 2.— Resonant scattering geometric function

We define a Doppler Dimming Function as

$$F_D(w) = \int_0^{+\infty} I_{ex}(\lambda - \delta\lambda)\,\Phi(\lambda, \mathbf{n'})\,d\lambda \quad (photons\ cm^{-3}\ s^{-1}\ sr^{-1}). \qquad (10)$$

This function should be integrated along the l.o.s., in fact the absorption profile varies because of the variation of the kinetic temperature in the direction of incident radiation, $T_{\mathbf{n'}}$, along the l.o.s., and also the shift, $\delta\lambda$, of the intensity exciting profile varies because of the different outflow velocities w along the l.o.s.
We know (Antonucci et al. 2000) that the heating of coronal ions is preferentially in the direction across the magnetic field, whereas in the radial direction, which is close to the direction of the incident radiation, $\mathbf{n'}$, the kinetic temperature remains close to the proton temperature (Figure 4), which do not varies too much with heliodistance.

Therefore we assume that the absorption profile is constant along the l.o.s. and for the kinetic temperature, which determines the width of that profile, we assume two extreme cases: a) isotropy, $T_{\mathbf{n'}} = T_{l.o.s.}$ and b) anisotropy, $T_{\mathbf{n'}} \sim T_e$ or $T_{\mathbf{n'}} \sim T_p \sim T_{HI}$??
In the following computations we use always the expression $F_D(w)$ that can assume two different values: $F_{D,is}(w)$ and $F_{D,an}(w)$ for isotropic and anisotropic hypothesis respectively.

In order to move out of the integral along the l.o.s. also the incident spectrum, $I_{ex}(\lambda - \delta\lambda)$, we point out that the outflow velocity, $\mathbf{w}$, has to be considered as an average velocity along the
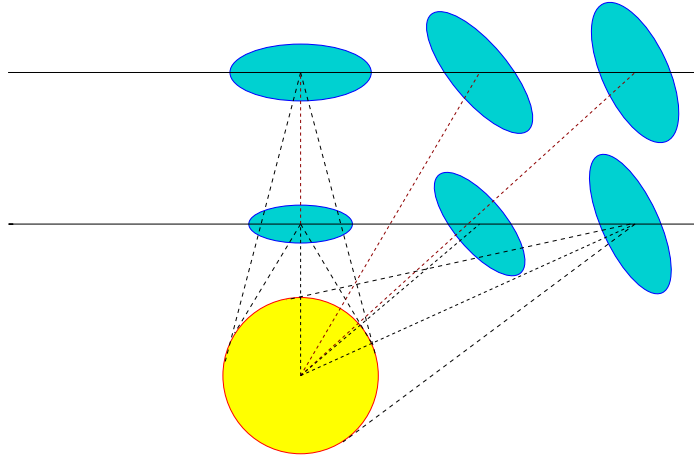
Fig. 3.— Incident radiation and absorption profiles at different height along the l.o.s.

l.o.s. Then by using equation 8 and 10 the radiative component, given by equation 1, becomes

$$I_r = \frac{b \ B_{12} \ h \ \lambda_0}{4\pi} \ \frac{\Omega}{4 \ \pi} \ F_D(w) \int_{l.o.s} n_i \, dl \ , \tag{11}$$

where the integral $\int_{l.o.s} n_i \, dl$ is the *column density* of the emitting ions/atoms along the l.o.s..

5. Collisional component approximations

As shown in the equation 7, q_{coll} depends on T_e, which in the polar coronal hole varies in the range between $10^6 K$ to $7 \times 10^5 K$ in the range of heliodistance considered. For example for O VI 1032 line with $T_e = 10^6 K$ we obtain $q_{coll} = 2.10 \times 10^{-8} cm^3 \ s^{-1}$, and with $T_e = 7 \times 10^5 K$ we obtain $q_{coll} = 2.28 \times 10^{-8} cm^3 \ s^{-1}$. (Figure 5). Therefore we assume q_{coll} constant along the l.o.s., with an uncertainty no more than 8%. Moreover for HI Lyα line, and similarly HI Lyβ line, as shown in Figure 5, the collisional coefficient is constant in the considered T_e range. For
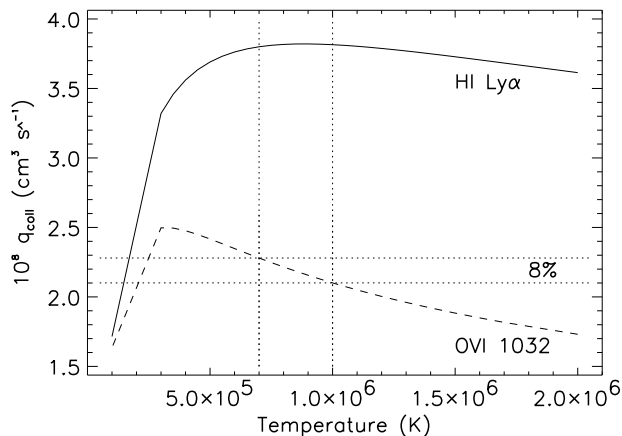

Fig. 4.— HI Lyα and OVI 1032 Collisional Coefficient as a function of the Electron Temperature

these reasons we write the collisional component, given in the equation 6, as

$$I_c \ \sim \ \frac{b}{4\pi} \ q_{coll} \int_{l.o.s} n_e \ n_i \, dl \ , \tag{12}$$

If we consider the "average" electron density along the l.o.s., $\langle n_e \rangle_i$, the previous equation can be written as [1]

$$I_c \sim \langle n_e \rangle_i \frac{b}{4\pi} q_{coll} \int_{l.o.s} n_i \, dl \; . \tag{13}$$

6. Separation of Collisional and Radiative Components

In order to separate the collisional and radiative contributions to a spectral line we need a pair of line from the same ion/atom indicated as a and b line, e.g for hydrogen we define the Lyα 1216 as the a line and the Lyβ 1025 as b line, while for oxygen: the lines at 1032 Å and 1037 Å are referred as a and b line respectively.

The observed intensities of a and b lines in the solar corona, $I_{obs,a}$ and $I_{obs,b}$, are the sum of the collisional and radiative components described in the previous sections therefore we can write

$$I_{r,a} + I_{c,a} = I_{obs,a} \; , \tag{14}$$

$$I_{r,b} + I_{c,b} = I_{obs,b} \; , \tag{15}$$

where $I_{r,a}$, $I_{c,a}$ and $I_{r,b}$, $I_{c,b}$ are the intensities of the radiative and collisional components of the a and b observed line, respectively.

We define the ratios, R_1 and R_2, of the radiative and collisional components of the two lines:

$$\frac{I_{r,a}}{I_{r,b}} = R_1 \; , \tag{16}$$

$$\frac{I_{c,a}}{I_{c,b}} = R_2 \; . \tag{17}$$

By using the approximate expression for the radiative component, given in equation 11, with indices a and b to denote the parameters of the two lines, we obtain [2]

$$R_1 = \frac{b_a}{b_b} \frac{B_{12,a}}{B_{12,b}} \frac{\lambda_{0,a}}{\lambda_{0,b}} \frac{F_{D,a}(w)}{F_{D,b}(w)} = \frac{b_a}{b_b} \frac{f_{12,a}}{f_{12,b}} \frac{\lambda_{0,a}^2}{\lambda_{0,b}^2} \frac{F_{D,a}(w)}{F_{D,b}(w)} \; . \tag{18}$$

On the basis of the approximate equation of the collisional component (equation 12) the ratio R_2 can be written as

$$R_2 = \frac{b_a}{b_b} \frac{q_{coll,a}}{q_{coll,b}} \; . \tag{19}$$

The ratio R_1 is function of the kinetic temperature, $T_{\mathbf{n'}}$, and the outflow velocity, w, through the function $F_D(w)$. The ratio R_2 is function of the atomic parameters and, through q_{coll}, of the electron temperature, T_e.

With the calculated ratios, R_1 and R_2, it is possible separate the components by solving the system given by the equations 14, 15, 16 and 17 therefore we obtain the collisional and radiative component of a and b observed lines as a function of the outflow velocity, w, with the following equations

---

[1] See section 6 for discussion about the quantity $\langle n_e \rangle_i$.

[2] For OVI lines $\lambda_{0,a}/\lambda_{0,b} \sim 0.995$ and $(\lambda_{0,a}/\lambda_{0,b})^2 \sim 0.989$, whereas for HI lines $\lambda_{0,a}/\lambda_{0,b} \sim 1.185$ and $(\lambda_{0,a}/\lambda_{0,b})^2 \sim 1.404$.

$$I_{r,b} = \frac{I_{obs,a} - R_2 \, I_{obs,b}}{R_1 - R_2} \; , \tag{20}$$

$$I_{c,b} = \frac{I_{obs,a} - R_1 \, I_{obs,b}}{R_2 - R_1} \; , \tag{21}$$

$$I_{c,a} = R_2 \, I_{c,b} \; , \tag{22}$$

$$I_{r,a} = R_1 \, I_{r,b} \; . \tag{23}$$

Note that in the case of OVI lines the ratio $\frac{F_{D,1032}(w)}{F_{D,1037}(w)}$ is a decreasing function of the outflow velocity, because of the pumping of the OVI 1037 Å line, therefore also the ratio R_1 is a decreasing function. Finally for this reason, by using equation 20, we can see that the radiative component of the OVI 1037 Å line increases with outflow velocity when is calculated from the separation of the line components. This fact has no physical meaning, but is due to the used diagnostics.

In the density code ($uv\_dens.pro$) the program to separate the components is $sep\_rad\_cll.pro$, in that program there are also the constraints on the line components that must be greater than zero, then we do not take into account the outflow velocity regions where these constraints are not satisfied.

6.1. Typical Values of R_1 and R_2

In the case of OVI lines, the ratio R_2 has a constant value because, by using equation 7, we can write

$$R_{2,OVI} = \frac{q_{coll,1032}}{q_{coll,1037}} \sim \frac{f_{12,1032}}{f_{12,1037}} = 2.02 \; . \tag{24}$$

For HI Lyα and HI Lyβ lines the ratio between the collisional coefficients varies no more than 1–2% around the value 5.52 (Figure 6), in the electron temperature range between $7 \times 10^5 K$ to $10^6 K$, therefore also for these lines R_2 can be considered constant

$$R_{2,HI} \sim \frac{1}{0.88} \, 5.52 = 6.27 \; . \tag{25}$$

Note: Raymond et al. (1997) found $I_{c,Ly\alpha}/I_{c,Ly\beta} = 7.57$ for logT=6.2, the difference with respect my value is about 20%. The increasing of the ratio between the two collisional coefficients is only few percent from logT=6.0 to logT=6.2 (Figure 6), therefore I don't know how to explain this difference, unless Raymond et al. (1997) compute the collisional coefficient in a different way.

To estimate the typical values of R_1 we can consider the static condition, $w = 0 \; km \; s^{-1}$. In this case by considering for both lines, a and b, the same absorption and exciting profiles [3] we can write the approximate expression:

$$\frac{F_{D,a}(0)}{F_{D,b}(0)} \sim \frac{\lambda_{0,b}}{\lambda_{0,a}} \frac{I_{disk,a}}{I_{disk,b}}, \tag{26}$$

---

[3]The absorption profiles of two lines from the same atom/ion have the same width if the profiles are considered in terms of thermal velocity,

$$\sigma_v = \sqrt{\frac{k_B \, T_{\mathbf{n}'}}{m_p \, A}} \; ,$$

but in terms of wavelength, σ_λ, given by equation 4, the width of the profiles depends on λ_0, therefore the approximation used in the equation 26 is strictly valid only when the functions $F_D(w)$ are obtained by integrating over the thermal velocity, whereas in this formulation $F_D(w)$ are obtained by integrating over the wavelength (equation 10).
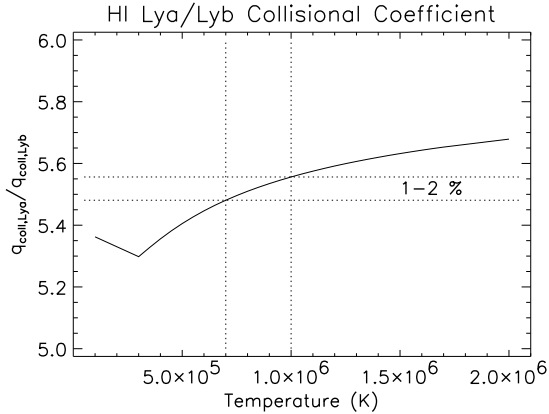
Fig. 5.— Ratio of HI Lyα and HI Lyβ Collisional Coefficients as a function of the Electron Temperature

where $I_{disk,a}$ and $I_{disk,b}$ are the total intensity of exciting radiation of a and b line, respectively [4].

Therefore the equation 18 in the static case can be written as

$$R_{1,OVI} \sim 2.01 \frac{I_{disk,1032}}{I_{disk,1037}}, \qquad (27)$$

$$R_{1,HI} \sim 7.09 \frac{I_{disk,Ly\alpha}}{I_{disk,Ly\beta}}, \qquad (28)$$

for OVI and HI lines, respectively. By using different disk intensity measurements (see Table 6) we obtain the values of R_1 reported in the following Table [5].

Table 4: Estimated Values of R_1 in static conditions with different disk intensities

disk →	Wilhelm	Raymond	Vernazza
$R_{1,OVI}$	4.18	4.00	4.00
$R_{1,HI}$	885	900	727

We can plot $R_{1,OVI}$ as a function of the outflow velocity, w, when the kinetic temperature is fixed, so we verify that $R_{1,OVI}(w)$ it is a decreasing function of w because of the pumping of the OVI 1037 Å line.

---

[4]With this approximation the expression of R_1, given in equation 18, can be written as

$$R_1 = \frac{b_a}{b_b} \frac{f_{12,a}}{f_{12,b}} \frac{\lambda_{0,a}}{\lambda_{0,b}} \frac{I_{disk,a}}{I_{disk,b}},$$

used by Marocchi, Antonucci and Giordano (2001).

[5]In coronal hole, where the absorption profile is usually very broad, $T_k \sim 10^7$ K, the ratio $R_{1,OVI}$ actually is always lower then 4.00, because of the pumping of $I_{r,1037}$ by CII 1037.02 Å line. The values of $R_{1,OVI}$ reported in Table 4 are obtained in coronal streamers or in coronal holes with anisotropic velocity distribution hypothesis.

7. "Average" electron density

From equation 13 we obtain the "average" electron density along l.o.s.

$$\langle n_e \rangle_i \sim \frac{I_{c,k} \, 4 \, \pi}{b_k \, q_{coll,k} \, \int_{l.o.s} n_i \, dl} \quad (cm^{-3}), \tag{29}$$

where $I_{c,k}$ is the collisional component, b_k is the branching ratio and $q_{coll,k}$ is the collisional coefficient of an observed k line. In our analysis we use as k lines the spectral line with not negligible collisional component, therefore the OVI 1032 Å or the HI Lyβ 1025 Å. The column density can be obtained from equation 11 by using spectral lines with dominant radiative component, therefore we use OVI 1032 Å or HI Lyα 1216 Å referred with index j,

$$\int_{l.o.s} n_i \, dl = \frac{I_{r,j} \, (4 \, \pi)^2}{b_j \, B_{12,j} \, h \, \lambda_{0,j} \, \Omega \, F_{D,j}(w)} \quad (cm^{-2}), \tag{30}$$

where $F_D(w)$ is a function of the average outflow velocity along the l.o.s. [6] . A quite strong approximation resides in the fact that the subtended solid angle, Ω, depends on the position along the line of sight.

Finally, by replacing the column density in the equation 29, the "average" electron density can be written as

$$\langle n_e \rangle_i \sim \frac{b_j \, B_{12,j} \, h \, \lambda_{0,j}}{b_k \, q_{coll,k}} \, \frac{\Omega}{4\pi} \, \frac{I_{c,k}}{I_{r,j}} \, F_{D,j}(w) \quad (cm^{-3}). \tag{31}$$

Some words are needed about the quantity $\langle n_e \rangle_i$. The usual definition of average value is

$$\langle n_e \rangle \stackrel{\text{def}}{=} \frac{\int n_e \, dl}{\int dl} \, , \tag{32}$$

but here we consider the "average" electron density weighted over the ion distribution along the l.o.s

$$\langle n_e \rangle_i = \frac{\int n_e n_i \, dl}{\int n_i \, dl} \, , \tag{33}$$

which by using equation 41 and assuming the ionization equilibrium of the coronal plasma along the l.o.s., can be approximated to

$$\langle n_e \rangle_i \sim \frac{\int n_e^2 \, dl}{\int n_e \, dl} = \frac{\langle n_e^2 \rangle}{\langle n_e \rangle} \, , \tag{34}$$

here we can see that, with this approximation, the quantity $\langle n_e \rangle_i$ is independent of the ion distribution, n_i, therefore we expect $\langle n_e \rangle_{OVI} = \langle n_e \rangle_{HI} = \langle n_e \rangle$, unless not ionization equilibrium, intensity calibration problems and/or filling factor effects and/or code bug (!?). The effect due to filling factor has to be discarded.

---

[6]The radiative and collisional components of a pair of lines are not independent, therefore the column density and also the electron density obtained is the same by using OVI 1037 Å instead of OVI 1032 Å or HI Lyβ 1025 Å instead of HI Lyα 1216 Å. In fact the ratio between the column density obtained by using a line ($I_{r,j} = I_{r,a}$) and b line ($I_{r,j} = I_{r,b}$) in equation 30 is equal to unity, as far as the electron density through the equation 31. This can be verified by using the following relation:

$$\frac{I_{r,a}}{I_{r,b}} = \frac{b_a}{b_b} \frac{B_{12,a}}{B_{12,b}} \frac{\lambda_{0,a}}{\lambda_{0,b}} \frac{F_{D,a}(w)}{F_{D,b}(w)} \, ,$$

obtained from equations 16 and 18.

From equation 31 and equations 20–23 we can study the behavior of the "average" electron density as a function of the observed intensities of a and b lines, $\langle n_e \rangle_i (I_{obs,a}, I_{obs,b})$. By considering the condition $R_1 > R_2$, which is everywhere satisfied for HI lines and for OVI lines it is satisfied for low outflow velocity $(w \leq 100 \ km \ s^{-1})$, we find that

$$\frac{\delta \langle n_e \rangle}{\delta I_{obs,a}} \ < \ 0$$

and

$$\frac{\delta \langle n_e \rangle}{\delta I_{obs,b}} \ > \ 0 \ .$$

7.1.   Relation Between $\langle n_e \rangle_{i,r_0}$ and $n_e(r_0)$

Here we draw an approximate relation between "average" electron density, $\langle n_e \rangle_{r_0}$, calculated at given heliocentric distance, r_0, and the electron density in the plane of the sky at the same height, $n_e(r_0)$. This relation can be calculated by using the definition of equation 34 and considering a spherical symmetric geometry with a known radial dependence of the electron density:

$$n_e(r) \ \propto \ r^{-b} \ , \tag{35}$$

where $b = 5, 4, 3, 2$, decreasing with heliocentric distance (Koutchmy 1977; Lallement, Holzer and Munro 1986; Gouttebroze et al. 1999). At a given heliocentric distance, r_0, in the plane of
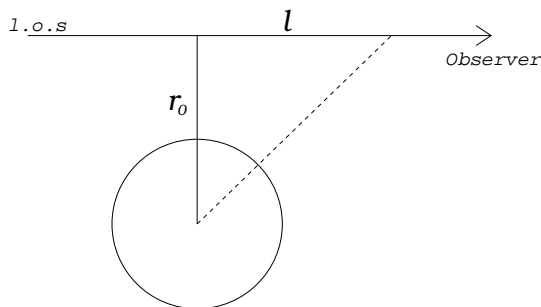
Fig. 6.— Line–of sight and radial direction

the sky, the electron density along the l.o.s. as a function of the distance, l, from the plane of the sky, can be written as

$$n_e(l, r_0) \ = \ n_e(r_0) \ \frac{r_0^b}{(l^2 + r_0^2)^{b/2}} \ , \tag{36}$$

the average value along the l.o.s., which is the quantity that we derive with our diagnostics, by following the definition of equation 34 is

$$\langle n_e \rangle_{i,r_0} \ = \ \lim_{N \to \infty} \frac{\int_0^{Nr_0} n_e^2(l, r_0) \ dl}{\int_0^{Nr_0} n_e(l, r_0) \ dl} \tag{37}$$

here by replacing $n_e(l, r_0)$ with equation 36 we obtain

$$\langle n_e \rangle_{i,r_0} \ = \ n_e(r_0) \ r_0^b \lim_{N \to \infty} \frac{\int_0^{Nr_0} \frac{dl}{(l^2+r_0^2)^b}}{\int_0^{Nr_0} \frac{dl}{(l^2+r_0^2)^{b/2}}} \ . \tag{38}$$

Table 5:

b	C_b	C_b^{-1}
2	0.50	2.00
3	0.59	1.70
4	0.625	1.60

Finally by solving the integrals with different values of b parameters we obtain

$$\langle n_e \rangle_{i,r_0} = C_b \, n_e(r_0) \,, \tag{39}$$

where the parameter C_b, reported in Table 5, is a constant value depending on b only.

8.   Element abundances

As Withbroe et al. (1982) we introduce the relation

$$n_i = \frac{n_i}{n_{el}} \frac{n_{el}}{n_H} \frac{n_H}{n_e} \, n_e \,, \tag{40}$$

where n_i is the ion density (density of element in "i" ionization state), n_{el} is the element density (summed over all the ionization states), n_H is the hydrogen density and n_e is the electron density. The term $n_i/n_{el} = C_i$ is the ionization fraction (atoms/ions concentration) and it is function of the electron temperature, T_e. The term n_{el}/n_H is the element abundance with respect to hydrogen. In the case of fully ionized atoms and He abundance equal to 10%, as typical coronal plasma condition, we have n_H/n_e=0.83. Therefore the equation 40 can be written as,

$$n_i = 0.83 \, \frac{n_{el}}{n_H} \, n_e \, C_i \,, \tag{41}$$

by using this relation, the resonantly scattered component, given by equation 11, can be written as

$$I_r \sim \frac{0.83 \, b \, B_{12} \, h \, \lambda_0}{4\pi} \frac{\Omega}{4\,\pi} F_D(w) \int_{l.o.s} \frac{n_{el}}{n_H} \, n_e \, C_i \, dl \,, \tag{42}$$

and the collisional component from equation 12 becomes

$$I_c \sim 0.83 \, \frac{b}{4\pi} \, q_{coll} \int_{l.o.s} \frac{n_{el}}{n_H} \, n_e^2 \, C_i \, dl \,. \tag{43}$$

The abundance, $\frac{n_{el}}{n_H}$, can be considered as constant along the l.o.s., moreover we assume that the plasma is in ionization equilibrium [7] along the l.o.s., that is C_i is constant, therefore the previous equations can be written as

$$I_r \sim \frac{0.83 \, b \, B_{12} \, h \, \lambda_0}{4\pi} \frac{\Omega}{4\,\pi} F_D(w) \frac{n_{el}}{n_H} C_i \int_{l.o.s} n_e \, dl \,, \tag{44}$$

$$I_c \sim 0.83 \, \frac{b}{4\pi} \, q_{coll} \, \frac{n_{el}}{n_H} C_i \int_{l.o.s} n_e^2 \, dl \,. \tag{45}$$

---

[7]The ionization equilibrium assumption is reasonable in streamers but it needs more discussion to be applicable in coronal holes.

We consider the radiative component of two observed spectral lines emitted one by ions, such as OVI ions ($\frac{n_{el}}{n_H} = \frac{n_O}{n_H}$), indicated as $I_{r,OVI}$, and the second one emitted by hydrogen atoms ($\frac{n_{el}}{n_H} = 1$), $I_{r,HI}$, then by computing the ratio between these two intensities represented by equation 44 we obtain

$$\frac{I_{r,OVI}}{I_{r,HI}} \sim \frac{b_{OVI}}{b_{HI}} \frac{B_{12,OVI}}{B_{12,HI}} \frac{\lambda_{0,OVI}}{\lambda_{0,HI}} \frac{F_{D,OVI}(w)}{F_{D,HI}(w)} \frac{n_O}{n_H} \frac{C_{OVI}}{C_{HI}} \ . \tag{46}$$

Finally we obtain the element abundance from the ratio of radiative components

$$\left(\frac{n_O}{n_H}\right)_r \sim \frac{I_{r,OVI}}{I_{r,HI}} \frac{b_{HI}}{b_{OVI}} \frac{B_{12,HI}}{B_{12,OVI}} \frac{\lambda_{0,HI}}{\lambda_{0,OVI}} \frac{F_{D,HI}(w)}{F_{D,OVI}(w)} \frac{C_{HI}}{C_{OVI}} \ , \tag{47}$$

where the index "OVI" can represent whether OVI 1032 Å or OVI 1037 Å line, and "HI" whether HI Lyα 1216 Å or HI Lyβ 1025 Å line [8] [9] .
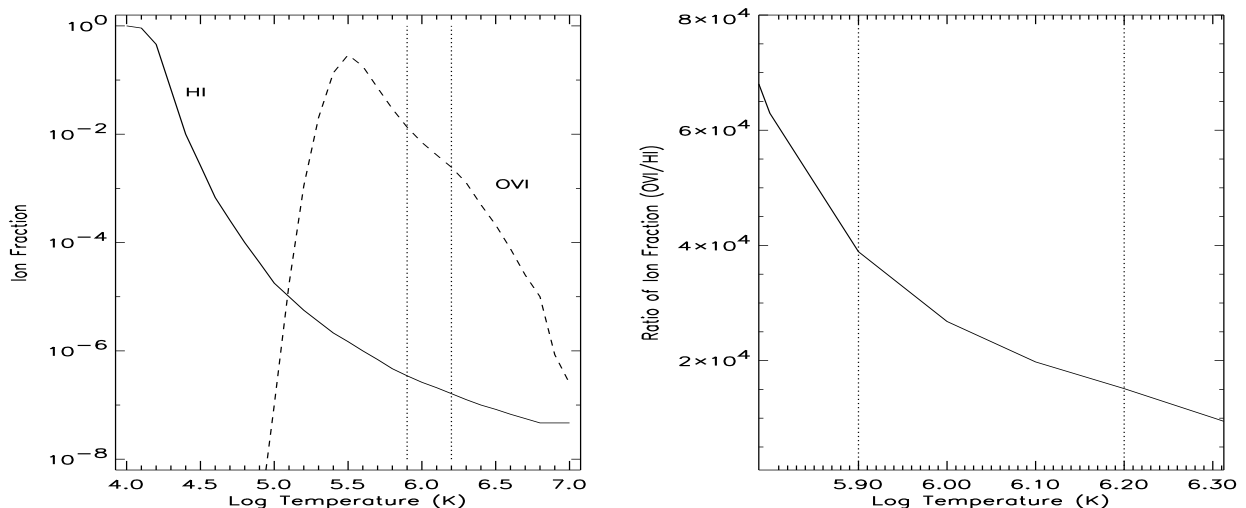

Fig. 7.— Neutral Hydrogen atom (HI) and Oxygen ions 5+ (OVI) fraction as a function of the Electron Temperature (left), ratio of the OVI and HI concentration in the temperature range between 8.0×10^5 K (5.90) and 1.6×10^6 K (6.20).

Similarly if we consider the collisional components, represented by equation 45, we obtain

---

[8]In any case, by using different choices: OVI 1032 Å or OVI 1037 Å and HI Lyα 1216 Å or HI Lyβ 1025 Å, we obtain exactly the same abundance. See also Note 6.

[9]In the case of static corona, and with strong approximations on absorption and exciting profiles, we can write

$$\frac{F_{D,HI}(0)}{F_{D,OVI}(0)} \sim \sqrt{\frac{A_{HI}}{A_{OVI}}} \frac{\lambda_{0,OVI}}{\lambda_{0,HI}} \frac{I_{disk,HI}}{I_{disk,OVI}} \ ,$$

where $\sqrt{\frac{A_{HI}}{A_{OVI}}} = \frac{1}{4}$, therefore the Oxygen abundance from radiative components becomes

$$\left(\frac{n_O}{n_H}\right)_r (0) \sim \frac{I_{r,OVI}}{I_{r,HI}} \frac{b_{HI}}{b_{OVI}} \frac{f_{12,HI}}{f_{12,OVI}} \frac{\lambda_{0,HI}}{\lambda_{0,OVI}} \frac{I_{disk,HI}}{I_{disk,OVI}} \frac{C_{HI}}{C_{OVI}} \frac{1}{4} \ ,$$

which, unless the term $\frac{\lambda_{Ly\beta}}{\lambda_{1032}} \sim 0.994$, is the same equation used by Raymond et al. (1997) and Marocchi, Antonucci and Giordano (2001), where $\frac{\delta\nu_{OVI}}{\delta\nu_{HI}} = \frac{1}{4}$.

the element abundance as

$$\left(\frac{n_O}{n_H}\right)_c \sim \frac{I_{c,OVI}}{I_{c,HI}}\frac{b_{HI}}{b_{OVI}}\frac{q_{coll,HI}}{q_{coll,OVI}}\frac{C_{HI}}{C_{OVI}} \ . \tag{48}$$

In these equations the concentration of ions with respect to the total density of the element is calculate, for given T_e, from ionization equilibrium curves by Arnaud and Rothenflug (1985) and Landini and Monsignori Fossi (1990) (Figure 8 left). The values of the ratio $\frac{C_{OVI}}{C_{HI}}$ are consistent with the value 15200 used by Marocchi, Antonucci and Giordano (2001), obtained at Temperature $Log(T_e) = 6.20$ (Figure 8 right).

Note that in literature the element abundance with respect to Hydrogen abundance, A_{el}, is usually given as

$$A_{el} = log\frac{n_{el}}{n_H} + 12 \tag{49}$$

with this notation the abundance $\frac{n_{el}}{n_H}$ is given by

$$\frac{n_{el}}{n_H} = 10^{A_{el}-12} \tag{50}$$

9. Doppler dimming function computation ...

In order to calculate for different lines the function $F_D(w)$ given in the equation 10, we need to know the intensity profile, $I_{ex}(\lambda)$, of the incident radiation from lower atmosphere, that is the chromospheric HI Lyα and HI Lyβ spectral lines and the OVI lines coming from the transition region. For every considered line the exciting spectrum has to satisfy the following relation:

$$\int_0^{+\infty} I_{ex}(\lambda) \, d\lambda \;=\; I_{disk} \; , \tag{51}$$

where I_{disk} is the total intensity measured by observing the solar disk. In the case of hydrogen lines the profiles used are those observed by Gouttebroze et al. (1978) (Figure 8) and the value of I_{disk} can be chosen from a set of different determination showed in Table 6. More recent measurements of the HI Lyα disk intensities and profiles have been performed by Lemaire et al. (2002) and described in the Appendix I. In the case of oxygen lines the possible choices of the measured total exciting intensity are also reported in Table 6. For the OVI lines profile shapes we use gaussian functions with the broadening observed by Warren et al. (1997), that for OVI 1032 Å corresponds to a temperature of 1.52×10^6 K (FWHM = 227 mÅ) and for OVI 1037 Å to 1.32×10^6 K (FWHM = 212 mÅ), a different choice is the assumption that the two OVI lines are formed at the same temperature (e.g. 1.52×10^6 K). In in case of OVI 1037 Å line we take into account also the two nearby CII lines at 1037.02 Å and 1036.34 Å. The intensities of these lines are given by Wilhelm et al. (1998) and reported in Table 6, the broadenings, corresponding to a temperature of 5.06×10^5 K (FWHM = 152 mÅ), are given by Warren et al. (1997).
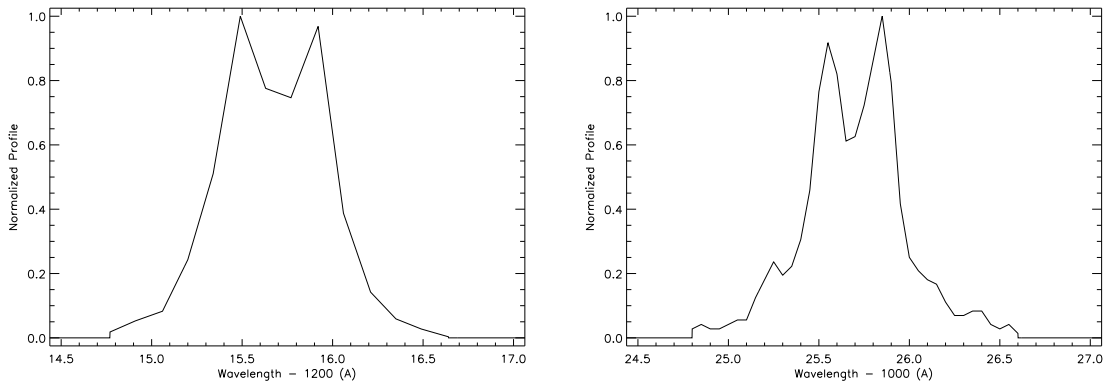

Fig. 8.— Left: Disk Intensity Profile of HI Lyα (left panel) and HI Lyβ (right panel).

For absorption profile, $\Phi(\lambda, \mathbf{n}')$, we need to make an assumption on the kinetic temperature along the direction of the incident radiation (equations 3 and 4), we consider the case of isotropic velocity distribution, $T_{n'} = T_{l.o.s.}$, and in the anisotropic case two different assumption on the kinetic temperature: $T_{n'} = T_e$ and $T_{n'} = T_p \sim T_{HI}$, we have to *verify* the differences in terms of n_e due to these assumptions for anisotropic case. *In the case of anisotropy the code is not correct, because does not take into account that the absorption profile is determined by electron temperature only in the radial direction (see fig 2 and fig 4), all the not-radial incident radiations over the subtended solid angle feel a velocity distribution that have a component due to l.o.s distribution.* Finally the function $F_D(w)$ is obtained for the velocity range between 0 to 600 $km \ s^{-1}$ by numerical integration of the equation 10 over the wavelength [10]

---

[10]To check the goodness of the numerical computation we can compare the Doppler dimming function numerically computed at $w = 0 \ km \ s^{-1}$ for the OVI 1032 Å line with the analytical solution of equation 10, which is

Table 6: Disk Intensities*

Spectral Line	A	B	C	D	E
H I Lyα	4.35×10^{15}	4.45×10^{15}	4.93×10^{15}	5.24×10^{15}	4.00×10^{15}
H I Lyβ			3.95×10^{13}	4.13×10^{13}	3.90×10^{13}
H I Lyγ			6.66×10^{12}	8.67×10^{12}	8.30×10^{12}
O VI 1032			1.29×10^{13}	1.94×10^{13}	1.60×10^{13}
O VI 1037			6.16×10^{12}	9.70×10^{12}	8.00×10^{12}
C II 1036			1.87×10^{12}		
C II 1037			2.33×10^{12}		
He II 304	1.11×10^{14}	3.83×10^{14}			

---

*(photons cm^{-2} s^{-1} sr^{-1})

[A] H I Lyα from Giordano (1998), He II 304 Quiet Sun from Brosius et al. (1996)

[B] H I Lyα from Lemaire et al. (1998), He II 304 Active Region from Brosius et al. (1996)

[C] Wilhelm et al. (1998)

[D] Raymond et al. (1997)

[E] Vernazza and Reeves (1978)

Examples of $F_D(w)$ functions computed for HI Lyα and Lyβ lines and for OVI 1032 Å and OVI 1037 Å lines are plotted in Figure 10. The used parameters relative to the incoming

---

possible for this line because both the exciting, $I_{ex}(\lambda)$, and the absorption, $\Phi(\lambda)$, profiles can be assumed to be gaussian. Therefore in this case the equation 10 for $w = 0 \ km \ s^{-1}$ becomes

$$F_{D,1032}(0) \; = \; \frac{I_{disk,1032}}{\sigma_{tot} \ \sqrt{2\pi}}. \tag{52}$$

where $I_{disk,1032}$ is the total disk intensity, and σ_{tot} is the quadratic sum, $\sigma_{tot} \; = \; \sqrt{\sigma_{\lambda,abs}^2 + \sigma_{\lambda,disk}^2}$, of the coronal absorption profile width, $\sigma_{\lambda,abs}$ (see equation 4) and the exciting profile width, $\sigma_{\lambda,disk}$. For example with $I_{disk,1032} = 1.94 \times 10^{13}$, $T_{n'} = T_{l.o.s.} = 2.42 \times 10^7$ and $T_{disk,1032} = 1.52 \times 10^6$ we obtain $F_{D,1032}(0) = 1.95 \times 10^{13}$ photons cm^{-2} s^{-1} sr^{-1} Å^{-1}, which has to be compare with the value obtained by code: $F_{D,1032}(0) = 1.91 \times 10^{13}$ photons cm^{-2} s^{-1} sr^{-1} Å^{-1}, OK. In the case of gaussian exciting and absorption profiles the equation 10 can be analytically integrated over the wavelength (λ) to obtain the following function of the outflow velocity (w):

$$F_{D,1032}(w) \; = \; \frac{I_{disk}}{\sigma_{tot} \ \sqrt{2\pi}} \ exp \left[-\frac{1}{2} \left(\frac{1}{\sigma_{\lambda,disk}} \frac{\lambda_0}{c} \mathbf{w} \right)^2 \right] exp \left[\frac{1}{2} \left(\frac{\sigma_{\lambda,abs}}{\sigma_{\lambda,disk}} \frac{1}{\sigma_{tot}} \frac{\lambda_0}{c} \mathbf{w} \right)^2 \right]. \tag{53}$$

We verified that the agreement between the analytical computation and the numerical solution is very good (see also test program $a\_n\_Dd.pro$ in the directory \$$HOME/PRO/UV_CODE/REPORT$).

Table 7: Disk Parameters used in the $F_D(w)$ functions computation

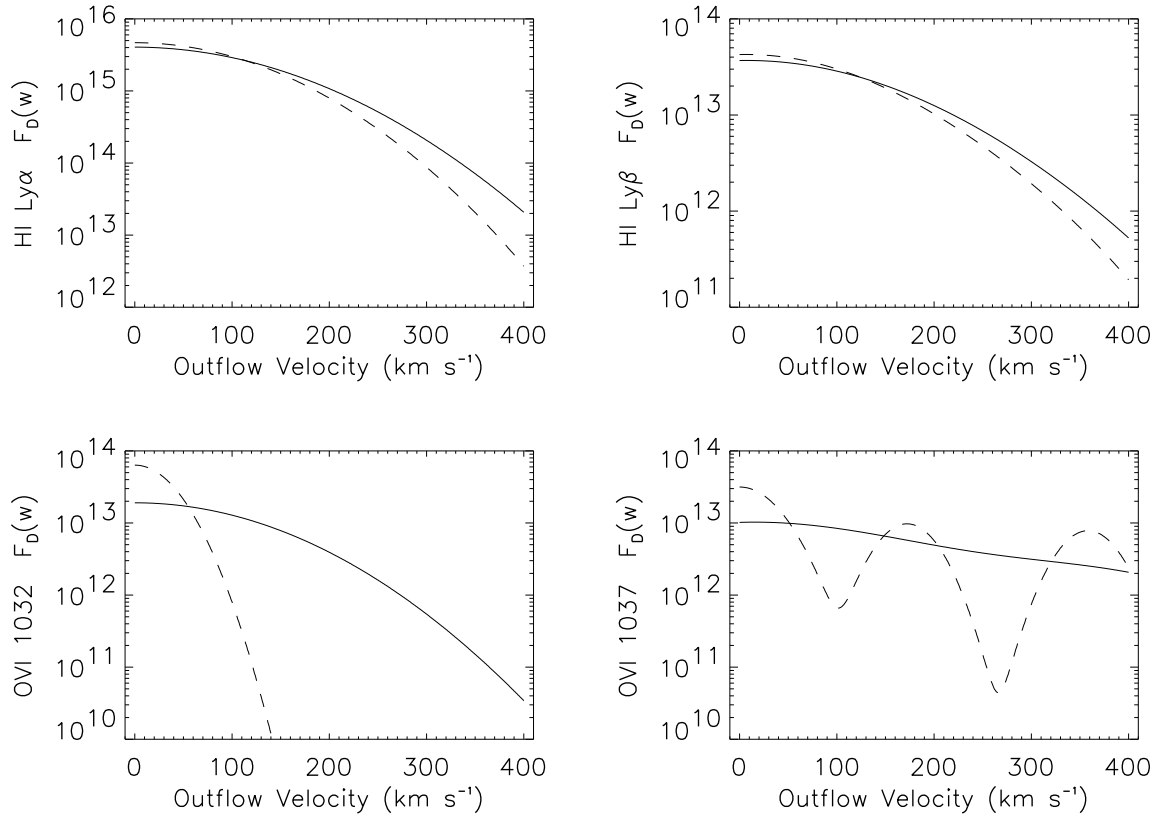| Line	Disk Intensity	Disk Profile
H I Lyα	Raymond et al. (1997)	Gouttebroze et al. (1978)
H I Lyβ	Raymond et al. (1997)	Gouttebroze et al. (1978)
O VI 1032	Raymond et al. (1997)	$T_{disk,1032} = 1.52 \times 10^6$
O VI 1037	Raymond et al. (1997)	$T_{disk,1037} = T_{disk,1032}$
C II 1036	Wilhelm et al. (1998)	$T_{disk,1036} = 5.06 \times 10^5$ *
C II 1037	Wilhelm et al. (1998)	$T_{disk,1037} = T_{disk,1036}$

---

*Warren et al. (1997)

Fig. 9.— Examples of $F_D(w)$ functions for HI Lyα, HI Lyβ, OVI 1032 Å and OVI 1037 Å lines. The solid curves are computed for isotropic case and dashed curves for maximum anisotropy.

disk radiation are reported in Table 7, whereas for kinetic temperature the observed values are reported in Table 8. The electron temperature, $T_e = 8.00 \times 10^5$, is extrapolated to this heliocentric distance from values obtained by David et al. (1998) at lower height. For every line we report the $F_D(w)$ function calculated for isotropic case (solid line, $T_{n'} = T_{l.o.s}$) and for maximum anisotropic case (dashed line, $T_{n'} = T_e$).

10.   Electron density computation ...

An example of the "average" electron density $\langle n_e \rangle_i$, computed by using the OVI lines as a function of the outflow velocity, for different heights in a Coronal Hole observed on May 1996, is reported in Figure 10. The physical parameters: line intensities and kinetic temperatures along the l.o.s., $T_{l.o.s.}$, observed by UVCS are in Table 8. We use the kinetic temperature of OVI 1032 line for OVI 1037 also. The outflow velocity acceptance region is determined by the conditions that both radiative and collisional components are greater that zero (see Section 5.)

Table 8: UVCS Observed parameters in a Coronal Hole

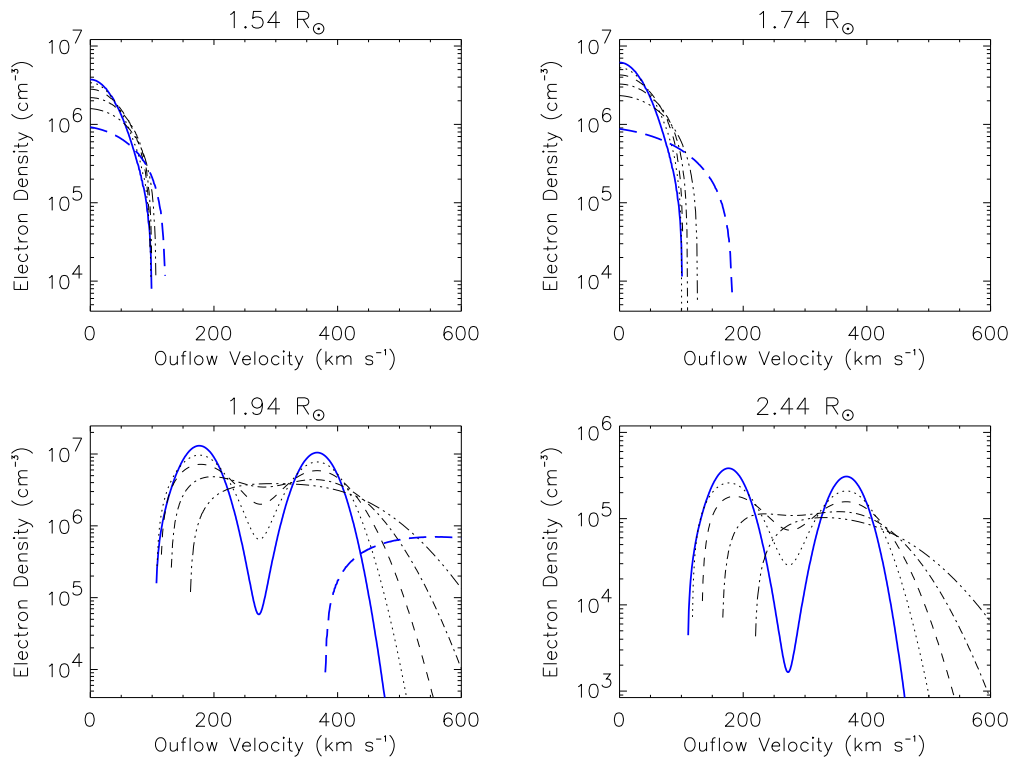| Height $(R_\odot)$	I_{1032} (*)	I_{1037} (*)	$T_{l.o.s,OVI}$ $(^\circ K)$
1.54	1.51×10^9	5.31×10^8	2.42×10^7
1.74	3.53×10^8	1.41×10^8	5.87×10^7
1.94	8.23×10^7	4.25×10^7	1.29×10^8
2.44	6.22×10^6	5.47×10^6	3.05×10^8

*(photons cm^{-2} s^{-1} sr^{-1})

Fig. 10.— Electron density as a function of outflow velocity at different heliocentric distance for radial kinetic temperature $T_{k,r}$ equal to T_e (bold solid lines), T_p (dotted lines), ($2 \times T_p$) (thin dashed lines), ($4 \times T_p$) (dot–dashed lines), ($8 \times T_p$) (triple dot–dashed lines), ($T_{l.o.s.}$) (bold dashed lines).

11. Expected HeII 304 intensity from observed HI Lyα

The expected intensity in a coronal streamer of the radiative component of HeII 304 in the solar corona can be evaluated with some approximations from the coronal observed intensity of the HI Lyα. The approximated radiative component of a coronal spectral line given by the Equation 11 can be written with an analytical formula, by assuming that the exciting and absorption profiles have both a gaussian shape (see Equation 53) and with the subtended solid angle approximation given by the equation 9. We can write the Einstein's coefficients as a function of the reference wavelengths ($\lambda_{0,HI}$, $\lambda_{0,HeII}$) with the Equation 5, and for the sake of simplicity we write the ratio between the radiative component of HI Lyα and HeII 304 lines in the case static case (Equation 53 with $w = 0$ becomes Equation 52):

$$\left(\frac{I_{HeII}}{I_{HI}}\right)_r \sim \frac{\lambda_{0,HeII}^2}{\lambda_{0,HI}^2} \frac{I_{disk,HeII}}{I_{disk,HI}} \frac{\sigma_{tot,HI}}{\sigma_{tot,HeII}} \frac{\int_{l.o.s} n_{HeII}\, dl}{\int_{l.o.s} n_{HI}\, dl} \tag{54}$$

The ions densities, n_{HI} and n_{HeII}, by using the Equations 40 and 41 we can written as

$$n_{HeII} = 0.83\, \frac{n_{He}}{n_H}\, C_{HeII}\, n_e, \tag{55}$$

$$n_{HI} = 0.83\, C_{HI}\, n_e, \tag{56}$$

where $\frac{n_{He}}{n_H}$ is the Helium abundance relative to the Hydrogen, the Neutral Hydrogen concentration, C_{HI}, and the Helium ions 1+ (HeII) concentration, C_{HeII}, as functions of Electron Temperature, T_e, are shown in Figure 11. By assuming a small variation of T_e along the l.o.s
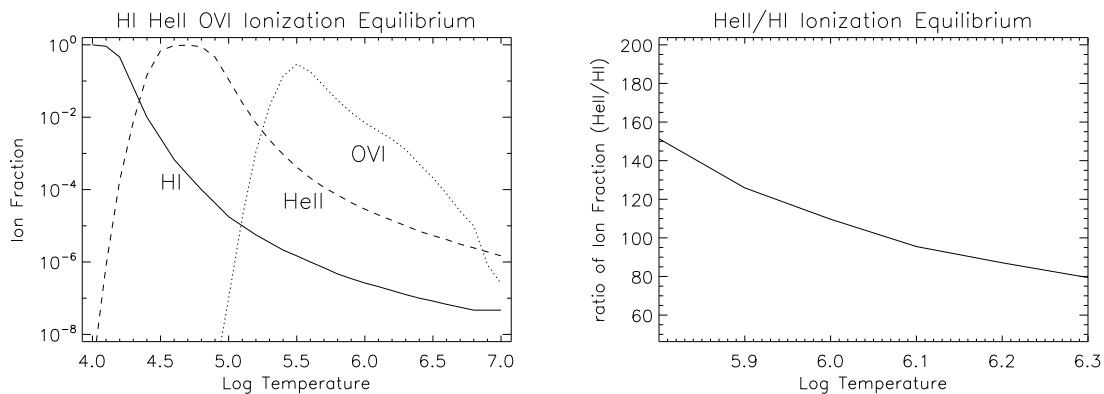

Fig. 11.— Left: Neutral Hydrogen atom (HI), Helium ions 1+ (HeII) and Oxygen ions 5+ (OVI) fraction as a function of the Electron Temperature. Right: Ratio of the HeII and HI concentration in the temperature range between 6.3×10^5 K (5.80) and 2.0×10^6 K (6.30).

we can consider an approximately constant ratio of the ions concentrations (see Figure 11 Right panel) and a constant Helium abundance, therefore we can drop out the integration along the l.o.s to obtain:

$$\left(\frac{I_{HeII}}{I_{HI}}\right)_r \sim \frac{\lambda_{0,HeII}^2}{\lambda_{0,HI}^2} \frac{I_{disk,HeII}}{I_{disk,HI}} \frac{\sigma_{tot,HI}}{\sigma_{tot,HeII}} \frac{n_{HeII}}{n_{HI}} \frac{C_{HeII}}{C_{HI}} \tag{57}$$

where the reference wavelengths, $\lambda_{0,HeII}$ and $\lambda_{0,HI}$, are given in Table 2, the disk intensities, $I_{disk,HeII}$ and $I_{disk,HI}$ in Table 6 (the expected disk ratio is in the range from 2.2×10^{-2} to 5.0×10^{-2}), the Helium abundance is estimated in the range from A_{He}=10.90 (Feldman 1992) to A_{He}=10.80 (Fludra and Schmelz 1999), therefore from $\frac{n_{He}}{n_H} = 7.9 \times 10^{-2}$ to $\frac{n_{He}}{n_H} = 6.3 \times 10^{-2}$,

assuming $T_e = 1.0 \times 10^6$ K the ionization ratio $\frac{C_{HeII}}{C_{HI}}$ is about 110 (see Figure 11 left panel), finally the parameters σ_{tot} are given by the following equation:

$$\sigma_{tot,HI} = \sqrt{\sigma^2_{\lambda,HI,abs} + \sigma^2_{\lambda,HI,disk}}$$

$$\sigma_{tot,HeII} = \sqrt{\sigma^2_{\lambda,HeII,abs} + \sigma^2_{\lambda,HeII,disk}}$$

where the standard deviation of the coronal gaussian profiles, $\sigma_{\lambda,abs}$, are related to the kinetic temperature with the Equation 4, and the width of the disk profiles, $\sigma_{\lambda,disk}$ are given by Brosius et al. (1996) for the HeII line (FWHM = 85.0 mÅ in the Quiet Sun and FWHM = 62.1 mÅ in the Active Region) and computed by a gaussian fitting of the HI Lyα line profile by Lemaire et al. (2002) (see Appendix I).

Assuming a Quiet Sun profile we have: $\sigma_{\lambda,HeII,disk} = 0.0360$ Å and $\sigma_{\lambda,HI,disk} = 0.34$ Å, and the ions coronal temperature equal to the electron temperature, $T_e = 1.0 \times 10^6$ K, we have $\sigma_{\lambda,HeII,abs} = 0.046$ Å and $\sigma_{\lambda,HI,abs} = 0.37$ Å, then we found $\frac{\sigma_{tot,HI}}{\sigma_{tot,HeII}} \sim 8.7$, and finally the expected intensity ratio of radiative components of HeII 304 and HI Lyα is

$$\left(\frac{I_{HeII}}{I_{HI}}\right)_r \sim 0.1 \div 0.2$$

In order to estimate the total intensity of the HeII 304 we have to take into account also the collisional component, while this component is negligible for the HI Lyα. An evaluation of the collisional HeII emission from a coronal streamer described with the Electron Temperature and Density given by Gibson and Fludra (1999) has been performed by Landini (2001) at 1.5R$_\odot$: $I_{HeII,c} \sim 4.0 \times 10^8$

We can perform the HeII intensity evaluation in a coronal streamer with a different assumption on the coronal ions temperature. By assuming as coronal temperature for the HI atoms the observed kinetic temperature in a coronal streamer below 2.0 R$_\odot$, $T_{k,HI} = 1.5 \times 10^6$ K, we have that $\sigma_{\lambda,HI,abs} = 0.45$ Å; for the HeII ions we assume an average temperature between the observed HI and OVI temperature, $T_{k,OVI} = 2.9 \times 10^6$ K, then $T_{k,HeII} = 2.2 \times 10^6$ K, from which we get $\sigma_{\lambda,HeII,abs} = 0.068$ Å, therefore we found $\frac{\sigma_{tot,HI}}{\sigma_{tot,HeII}} \sim 7.3$. In this case the radiative intensity of the HeII line is reduced of about 20 % with respect the previous evaluation. Finally assuming the same temperature for OVI and HeII ions the intensity reduction is anyhow lower then 30 %.

$$\left(\frac{I_{HeII}}{I_{HI}}\right)_r \sim 0.07 \div 0.16$$

12.   Appendix I – HI Lyα disk profiles

Recent measurements of the HI Lyα disk intensities and profiles have been performed by Lemaire et al. (2002) from SUMER observations at different periods of the solar cycle activity from Jul 1996 to Aug 2001.

The code used to compute the HI Lyα disk profiles is *read_lyaprof.pro* and the data are for example *Lalpha_May2000_20.data* in the directory $*HOME/PRO/UV_CODE/REPORT/HI_DISK_LEMAIRE2002.*
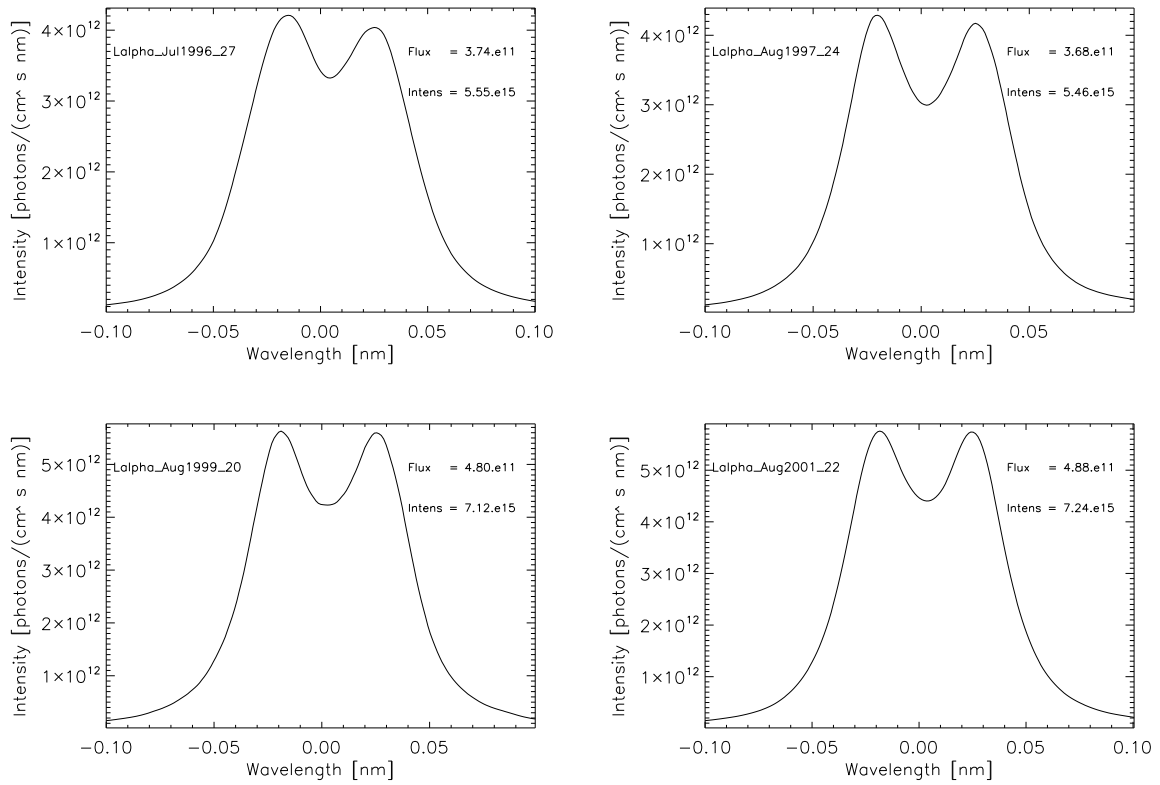

Fig. 12.— Sample of the HI Lyα disk intensity profiles from Lemaire et al. (2002)

REFERENCES

Antonucci, E., Dodero, M.A. and Giordano, S.: 2000, *Sol. Phys.*, in press.

Antonucci, E., Giordano, S., KrishnaKumar, V. and Noci, G.: 2001, *A&A*, submitted.

Arnaud, M. and Rothenflug, R.: 1985, *A&ASuppl. Ser.*, 60, 425.

Beckers, J.M., and Chipman, E.: 1974, *Sol. Phys.*, 34, 151.

Brosius, J.W.: 1996, *ApJSuppl. Ser.*, 106: 143–164.

David, C., Gabriel, A.H., Bely-Dubau F., Fludra, A., Lemaire, P. and Wilhelm, K., 1998, *A&A*, 336, L90–94.

Feldman, U., Mandelbaum, P., Seely, J.L., Doschek, G.A., Gursky H., 1992, *ApJS*, 81, 387

Fludra, A., and Schmelz, J. T.; 1999, *AA*, 348, 286

Foukal, P.V.: 1990, *"Solar Astrophysics" John Wiley & Sons, Inc*, pag 93.

Gibson, S.E., and Fludra, A.: 1999, *JGR*, 104, 9691.

Giordano, S.: 1998, *PhD Thesis, University of Torino.*

Gouttebroze, P., Lemaire, P., Vial, J.C., and Artzner, G.: 1978, *"The solar hydrogen Lyman-alpha and Lyman-beta lines - Disk center observations from OSO 8 compared with theoretical profiles"*, *ApJ*, 225, 655.

Guhathakurta, M., Fludra, A., Gibson, S. E., Biesecker, D. and Fisher, R.: 1999, *JGR*, 104, A5, 9801–9808.

Koutchmy, S., 1976, *Sol. Phys.*, 51, 399–407.

Lallement, R., Holzer, T.E.and Munro, R.H., 1986, *JGR*, 91, A6, 6751–6759.

Landini M. and Monsignori Fossi, B.C.: 1990, *A&ASuppl. Ser.*, 82, 229–260.

Landini M. : 2001, *private communication.*

Lang, K.R.: 1978, *"Astrophysical Formulae" Springer–Verlag*, pag 90.

Lemaire, P., Emerich, C., Curdt, W., Schülhe, U. and Wilhelm, K.: 1998, *A&A*, 334, 1095–1098.

Lemaire et al.: 2002, *ESA SP - SOHO 11*, 219

Marocchi, D., Antonucci, E. and Giordano, S.: 2001, *Annales Geophysicae*, 19, 135–145.

Mewe, R.: 1972, *A&A*, 20, 215–221.

Noci, G., Kohl, J.L. and Withbroe, G.L.: 1987, *ApJ*, 315, 706.

Noci, G., Poletto, G. Suess, S.T., Wang, A.-H. and Wu, S.T.: 1993, *Sol. Phys.*, 147, 73–96.

Raymond, J.C., Kohl, J.L., Noci, G., Antonucci, E., Tondello, G., Huber, M.C.E., Gardner, L.D., Nicolosi, P., Fineschi, S., Romoli, M., Spadaro, D., Siegmund, O.H.W., Benna, C., Ciaravella, A., Cranmer, S., Giordano, et al., L.: 1997, *"Composition of the coronal streamers from the SOHO Ultraviolet Coronagraph Spectrometer" Sol. Phys.*, 175, 645–665.

Rybicki, G.B. and Lightman, A.P.: 1979, *"Radiative Process in Astrophysics" John Wiley & Sons, Inc*, pag 275.

Vernazza J.E. and Reeves, E.M.: 1978, *ApJS*, 37, 485-513.

Withbroe, G.L., Kohl, J.L., Weiser, H. and Munro, R.H.: 1982, *Space. Sci. Rev.*, 33, 17.

Warren, H.P., Mariska, J.T., Wilhelm, K., and Lemaire, P.: 1997, *ApJ*, 484, L91.

Wilhelm, K., Lemaire, P., Dammasch, I.E., Holland, J., Schülhe, U., Curdt, W., Kucera, T., Hassler, D.M. and Huber, M.C.E.: 1998, *A&A*, 334, 685.